SUPPORTING INFORMATION

Linear assembly of lead bromide-based nanoparticles inside lead(II) polymers prepared by mixing the precursors of both the nanoparticle and the polymer

Soranyel Gonzalez-Carrero,[a] Lorena Bareño, [a] Elke Debroye,[b] Cristina Martin,[b] Patricia Bondia,[c] Cristina Flors, [c] Raquel E. Galian,[a] Johan Hofkens[b,*] and Julia Pérez-Prieto[a,*]

[a]Instituto de Ciencia Molecular (ICMoL), Universidad de Valencia, Catedrático José Beltrán 2, 46980, Paterna, Valencia, Spain.

[b]Department of Chemistry, KU Leuven, Celestijnenlaan 200F, B-3001, Leuven, Belgium

[c]Madrid Institute for Advanced Studies in Nanoscience (IMDEA Nanociencia), Faraday 9, 28049, Madrid, Spain

EXPERIMENTAL SECTION

Materials

Lead bromide (99.999 %), methylamine (40 % in water), cyclohexanemethylamine (98 %), dimethylformamide (99.8 %) and hydrobromic acid (47 %), were purchased from Sigma-Aldrich. The organic solvents used were spectroscopic grade (Sharlab). Methylammonium bromide (CH_3NH_3Br; MABr) and cyclohexanemethylamonium halide ($C_6H_{11}CH_2NH_3Br$; ChMABr) were synthesized by reaction of the corresponding amine in water/acid.

Synthesis of $MAPbBr_3$ colloidal nanoparticles

The $MAPbBr_3$ nanoparticles were synthesized using a re-precipitation method. A dimethylformamide precursor solution was prepared by mixing methylammonium bromide (MABr, 10 mg/mL, 28 µL, 2.6 µmol), lead bromide ($PbBr_2$, 10 mg/mL, 100 µL, 2.7 µmol) and the ligand (ChMBr, 1.7 mg/mL, 22 µL, 0.19 µmol), the molar ratio between $PbBr_2$:MABr:ChMABr components was 1:0.93:0.07. The precursor solution was added dropwise to toluene (5mL) and stirred for 60 minutes, at room temperature. The yellow toluene dispersion was allowed to stand for 24 hours, and finally the supernatant with the colloidal nanoparticles was separated and the solid discarded. The nanoparticles were maintained as colloidal solution in toluene.

Synthesis of $PbBr_2$ nanoparticles

Control assays were carried out in the absence of MABr under the same conditions described above. First, a dimethylformamide precursor solution was prepared by mixing lead bromide ($PbBr_2$, 10 mg/mL, 100 µL, 2.7 µmol) with the ligand (ChMBr, 1.7 mg/mL, 22 µL, 0.19 µmol), with a $PbBr_2$:ChMABr molar ratio of 1:0.07. Then, the precursor solution was added dropwise to toluene (5mL) and stirred for 60 minutes, at room temperature. The white solution was allowed to stand for 24 hours, and finally the supernatant was separated and the solid discarded.

Characterization

Optical measurement. UV-visible spectra of the colloidal nanoparticles were recorded in a UV-visible spectrophotometer secoman Uvi Ligth XT5. Steady-state PL spectra were measured on an Amnico Browman series 2 Luminescence spectrometer, equipped with a Xenon lamp (150 W). The AB2 software (v. 5.5) was used to register the data. The UV-Vis absorption spectra of samples deposited on hydrophobic glass were recorded in a JASCO V-670 spectrometer with horizontal integrating sphere (PIV-757).

The PL quantum yield of colloidal nanoparticles (in toluene) was performed in a Hamamatsu C9920-02 absolute PL Quantum Yield Measurement System, with monochromatic light source (150 W) and integrating sphere. All the data were acquired using 1cm×1cm path length quartz cuvettes, at room temperature, using an excitation wavelength of 365 nm.

Time-resolved PL decay kinetics of colloid and the samples deposited on hydrophobic glass were measured using a compact fluorescence lifetime spectrometer C11367, Quantaurus-Tau, with a diode pulse light source of 470 nm. Fluorescence lifetime software U11487 was used to register the data. The PL decays of colloidal perovskite nanoparticles were fitted with a triexponential function. The average lifetimes (τ_{av}), were calculate as $\tau_{av} = \Sigma A_i\tau_i^2 / \Sigma A_i\tau_i$; where τ_i are the decay times and α_i represents the amplitudes of the components, values obtained from the fitted PL kinetic decay traces.

Morphology characterization.

Transmission electron microscopy (TEM) images were acquired using a Jeol 1010 microscope operating at 80 kV equipped with a charge-coupled device (CCD) camera. Scanning electron microscopy (SEM) images of nanoparticles deposited on glass were obtained using a HITACHI S-4800 with a spotlight of field emission gun. Images were acquired using an acceleration voltage of 10 kV. A gold/palladium coating was used for perform the measurement of nanoparticles deposited on glass. The Energy dispersive X-ray spectroscopy spectra was acquired on HITACHI S-4800 equipped with XFlash 5030 Bruker detector and acquisition software QUANTAX 400.

Preparation of samples on TEM grid

The TEM grid was prepared by placing 30 µL of fresh $MAPbBr_3$ colloid dropwise on a carbon-coated copper TEM grid. The sample deposited on the TEM grid was evaporated slowly inside a vial exposed to hexane saturated atmosphere at room temperature.

Powder X-Ray Diffraction (PXRD).

The PXRD analyses was performed in a powder diffractometer D8 Advance A25 model Bruker, with a powder diffractometer θ-θ configuration, X-ray tubes on a lineal receiver Cu radiation. Plus DIFFRAC EVA Data assessment program was used to register the data. The diffracted intensities were recorded, at room temperature, from 5° to 80° 2θ angles using a step size of 0.02°.

Thermogravimetry analysis (TGA).

The colloidal nanoparticles obtained after synthesis were precipitated by centrifugation (at 10000 rpm) and the resulting powder was analyzed by TGA. A Mettler Toledo TGA/SDTA 851e system, with an operative temperature of 25–800 °C (rate of 10 °C min^{-1}) and under a nitrogen flux (40 mL min^{-1}) was used for the measurement.

Nuclear magnetic resonance (^{1}H-NMR).

The quantification of the organic cations in the perovskite nanoparticles was performed by using ^{1}H-NMR. First, the colloidal nanoparticles obtained after synthesis were precipitated by centrifugation (at 10000 rpm) and the resulting powder was reverted back into the precursors by dissolving it in deuterated dimethyl sulfoxide. Then, the spectra were registered at room temperature in a Bruker DPX300 spectrometer, with a 300 MHz Bruker magnet (7 T). The chemical shifts (δ) are reported in ppm relative to tetramethylsilane. Finally, the composition of the perovskite nanoparticles was possible by combining these results with the contribution of the inorganic material (i.e. $PbBr_2$) in the TGA.

The X-ray photoelectron spectroscopy (XPS)

The analysis of nanoparticles surface was carried out by using a K-ALPHA Thermo Scientific. The spectra were collected using monochromatized Al-K radiation (1486.6 eV), yielding a focused X-ray spot (elliptical in shape with a major axis length of 400µm) at 3 mA and 12 kV. The alpha hemispherical analyser was operated in the constant energy mode with survey scan pass energies of 200 eV to measure the whole energy band and 50 eV in a narrow scan to selectively measure of elements studied.

Atomic force microscopy (AFM).

The topographic measurement of nanoparticles deposited on hydrophobic glass was performed on an atomic force microscope Agilent Systems Pico LEI-I, equipped with a silicon probe (tip radius 7 nm), using a resonance frequency of 300 kHz and a spring constant of 26.1 Nm^{-1}. The images were acquired in tapping mode under ambient conditions using Picoview software (version 2.0) for data acquisition. The samples were prepared on a hydrophobic glass slide (22 mm x 22 mm).

Device preparation.

The indium tin oxide (ITO) coated glass used as substrate were cleaned ultrasonically in alkaline detergent (Hellmanex solution), water, acetone and isopropanol baths. After dry, the ITO subtracted were placed in a UV-ozone claner (30 min). Thereafter, the ITO substrate was coated with a solution of the hot injection layer, PEDOT:PSS (Sigma Aldrich), by spin coating at 3000 rpm for 120 s and the annealed at 150˚C during 15 min. Followed by the $MAPbBr_3$ thin layer, which was prepared by spin coated from toluene dispersion at 1500 rpm for 60 s and annealed for 15 min at 80 ˚C. Finally, the injection layer of 2-(4-tert-Butylphenyl)-5-(4-biphenylyl)-1,3,4-oxadiazole (PBD, Sigma Aldrich) in cyclohexane was spin coated at 5000 rpm for 120 s and annealed at 80˚C. The Al electrode was vapour deposited on top of the organic layer. The Current-density–voltage (J–V) curve were measured in the dark at room temperature using a Keihtley 2400 device.

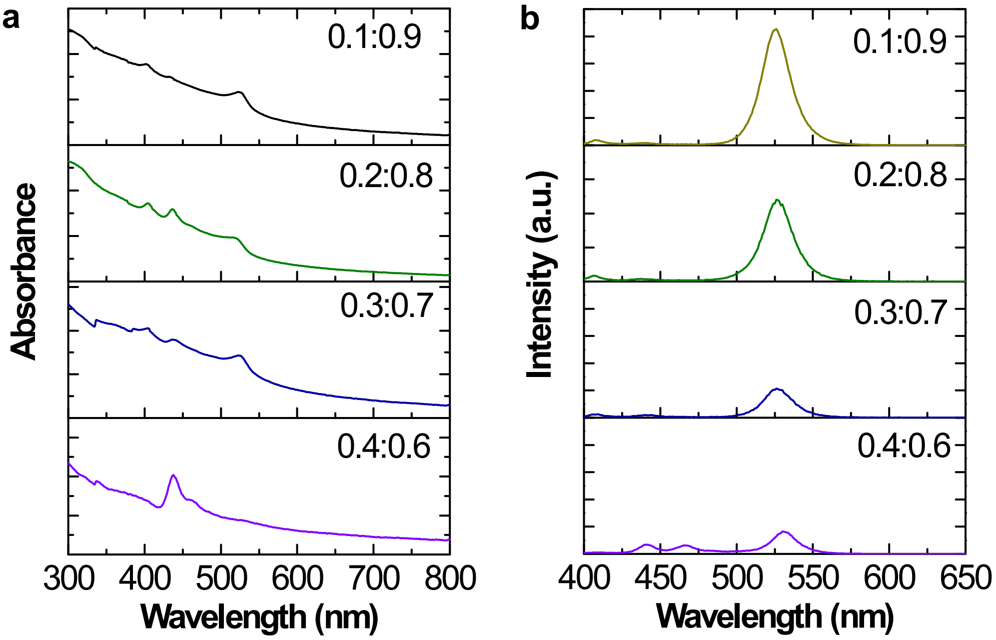

Figure S1. a) Absorption and b) emission spectra of toluene dispersion of perovskite synthesised at different alkyl ammonium salt ChMABr:MABr molar ratio.

Table S1. Time-resolved PL measurements of the $MAPbBr_3$ colloid used for the studies and 10-fold diluted colloid

$MAPbBr_3$	**PL[a]**	**τ_{av} [a] (ns)**	**τ_1 (ns)**	**τ_2 (ns)**	**τ_3 (ns)**	**A_1 (%)**	**A_2 (%)**	**A_3 (%)**
Concentrated colloid	530	769	26	167	977	39	38	23
Diluted colloid	530	339	17	115	539	63	28	10

[a] *Excitation wavelength at 470 nm*

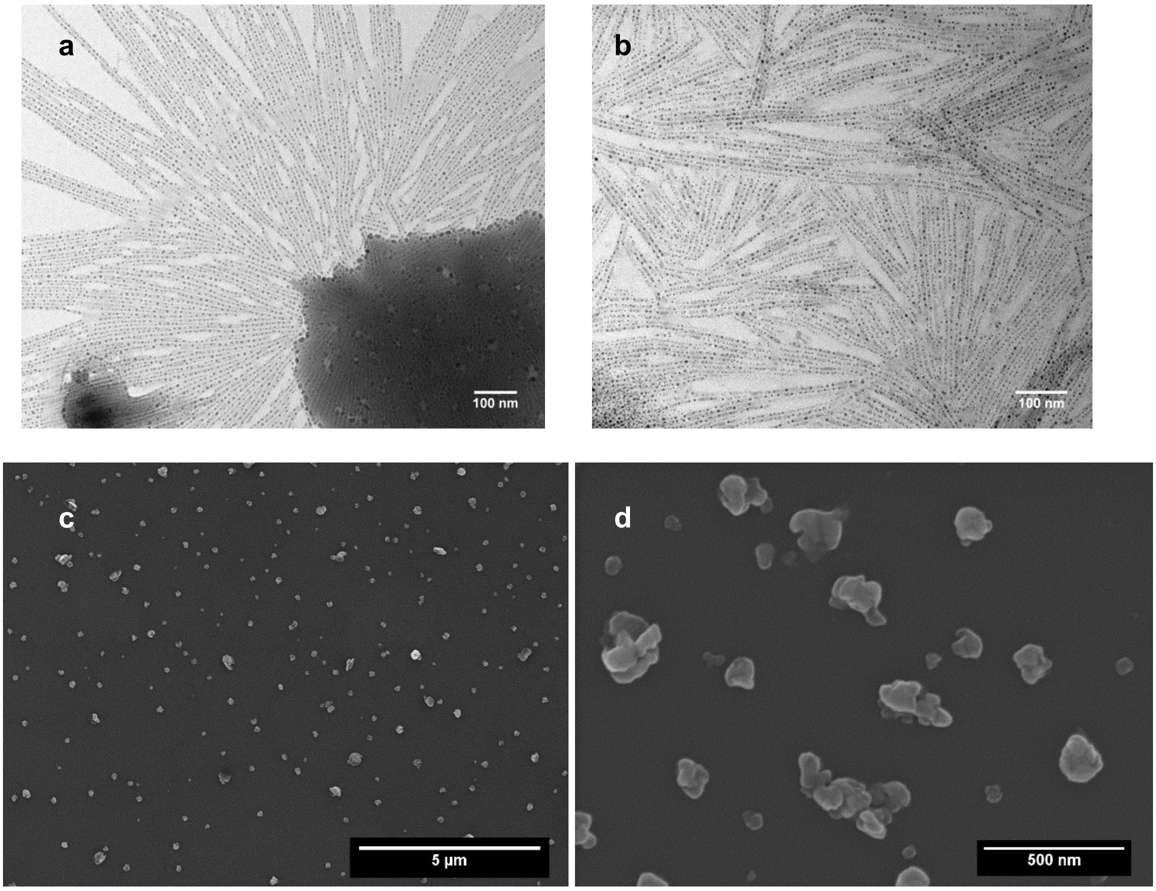

Figure S2. a,b) TEM image of control sample showing the formation of similar 1D polymer-like chains of several microns in length but containing $PbBr_2$ nanoparticles; scale bar 100 nm. c,d) SEM images of $\text{cNP}_{\text{oligomer}}$ from the control sample deposited on hydrophobic glass. Scale bar 5 µm and 500 nm.

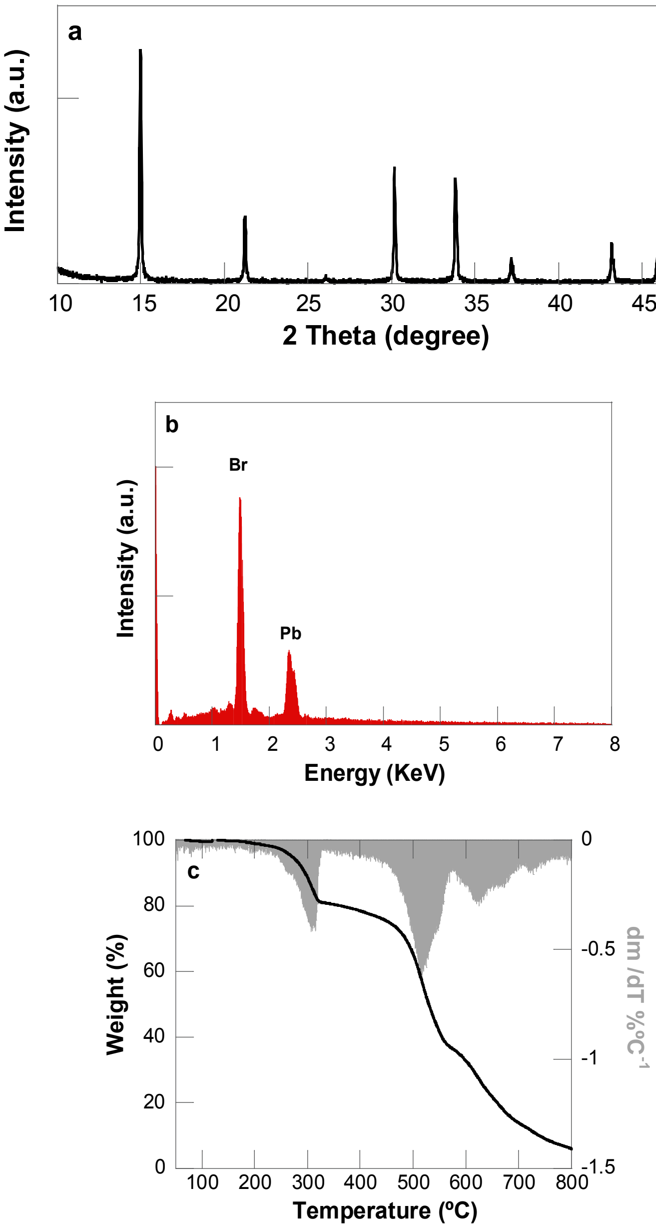

Figure S3. a) PXRD and b) energy dispersive diffraction spectra of $MAPbBr_3$. c) TGA heating curves (black line) and the corresponding 1st derivatives (grey shadow) of $MAPbBr_3$.

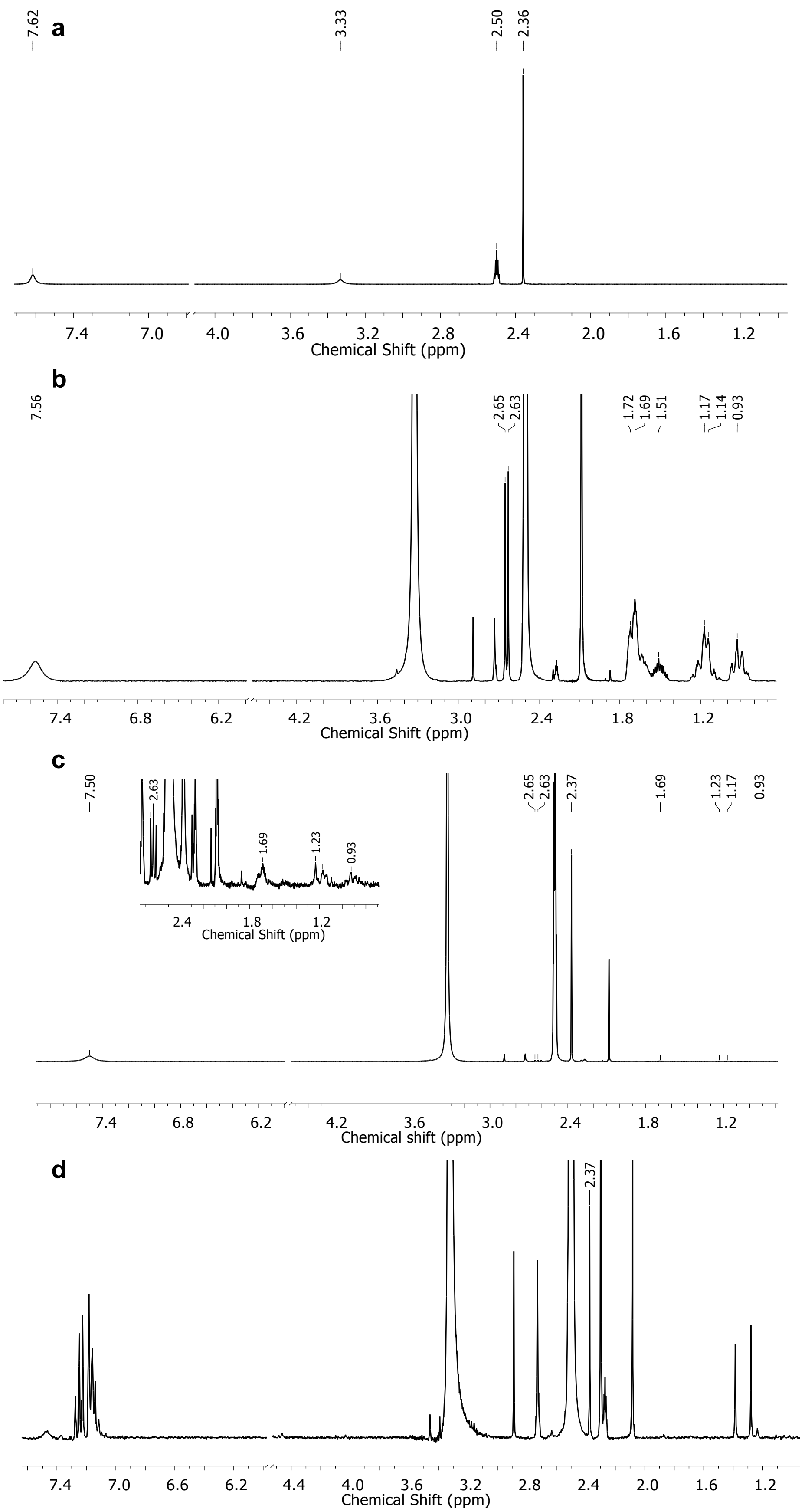

Figure S4. ^{1}H-NMR spectra of: a) MABr, b) ChMABr, c) $MAPbBr_3$ nanoparticles and d) the bulk solid precipitated after synthesis in deuterated dimethyl sulfoxide. Inset image c: zoom of selected area.

X-ray photoelectron spectroscopy analysis

X-ray photoelectron spectroscopy (XPS) analysis was performed to gain further insight into the components of the 1D assemblies. Figures S5 and S6 show the XPS spectra of Pb 4f, Br 3d and N 1s of the 1D $MAPbBr_3$ NP polymer and those of the sample prepared in the absence of MABr, i.e., the 1D $PbBr_2$ NP polymer (C1s at 284.6 eV was used as the internal reference for the analysis). The Pb 4f XPS spectrum of both polymers shows the two symmetrical peaks at 138.2 and 143.1 eV attributed to Pb $4f_{7/2}$ and Pb $4f_{5/2}$, respectively.[1, 2] The Br 3d spectrum showed two peaks centred at 67.7 eV and 67.9 eV, which are characteristic of both $MAPbBr_3$ and $PbBr_2$,[3, 4] together with two other lower intensity bands centred at 66.1 and 67.0 eV, which can be ascribed to the lead(II) coordination polymer. The N 1s spectrum of the 1D $MAPbBr_3$ NP polymer shows two peaks at 399.7 eV and 401.6 eV, which can be ascribed to cyclohexanemethylamine and methylammonium, respectively.[2, 5] In fact, the 1D $PbBr_2$ NP polymer only shows the peak ascribed to cyclohexanemethylamine.

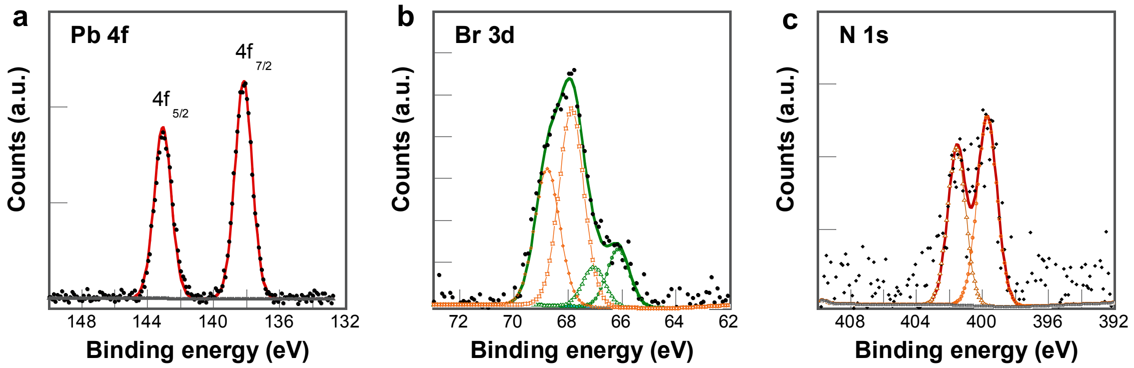

Figure S5. XPS spectra of Pb 4f, Br 3d and N 1s of the 1D $MAPbBr_3$ NP polymer

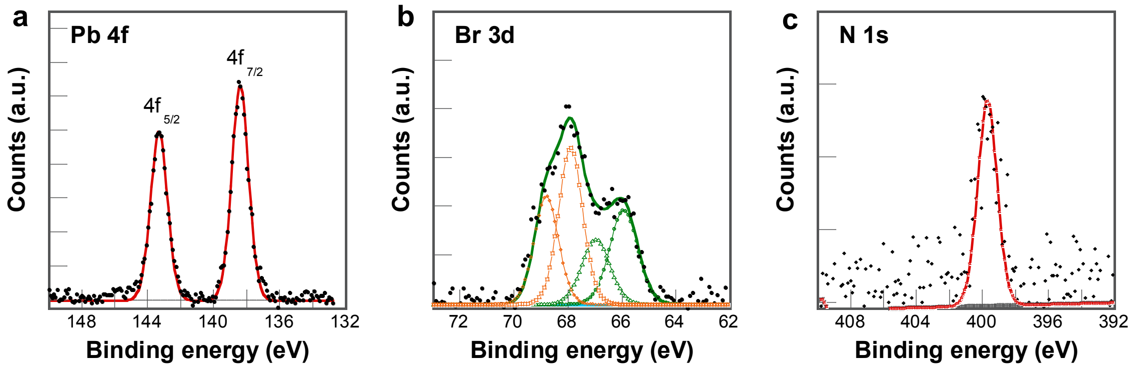

Figure S6. XPS spectra of Pb 4f, Br 3d and N 1s of the 1D $PbBr_2$ NP polymer prepared in the absent of MABr.

Correlative AFM and fluorescence microscopy

The sample was prepared by drop casting of 100 µL of $MAPbBr_3$ in toluene on a clean cover glass (Menzel-Gläser 22 mm ∅, #2). The correlative AFM and fluorescence microscopy was carried out on an adapted setup that integrates AFM (Nanowizard II, JPK Instruments) on a standard inverted optical microscope (Nikon Eclipse Ti).[6, 7] Wide-field illumination was achieved by focusing the expanded and collimated laser beam (488 nm, 10 $W\cdot cm^{-2}$ at the sample, Luxx, Omicron) onto the back focal plane of the objective (TIRF, 60x, 1.49 NA, oil immersion, Nikon). The emission passes through a dichroic mirror (488 nm) and two additional spectral filters (HQ500 LP, HQ525/50, Chroma Technology) and is detected by using an EMCCD camera (iXon Ultra 897, Andor Technology). An integration time per frame of 124 ms and a total number of 1000 frames were collected. The topographic AFM image of the same region of interest was registered in tapping mode (HQ:NSC35, tip radius 8 nm). The data were analysed by using Andor Solis software.

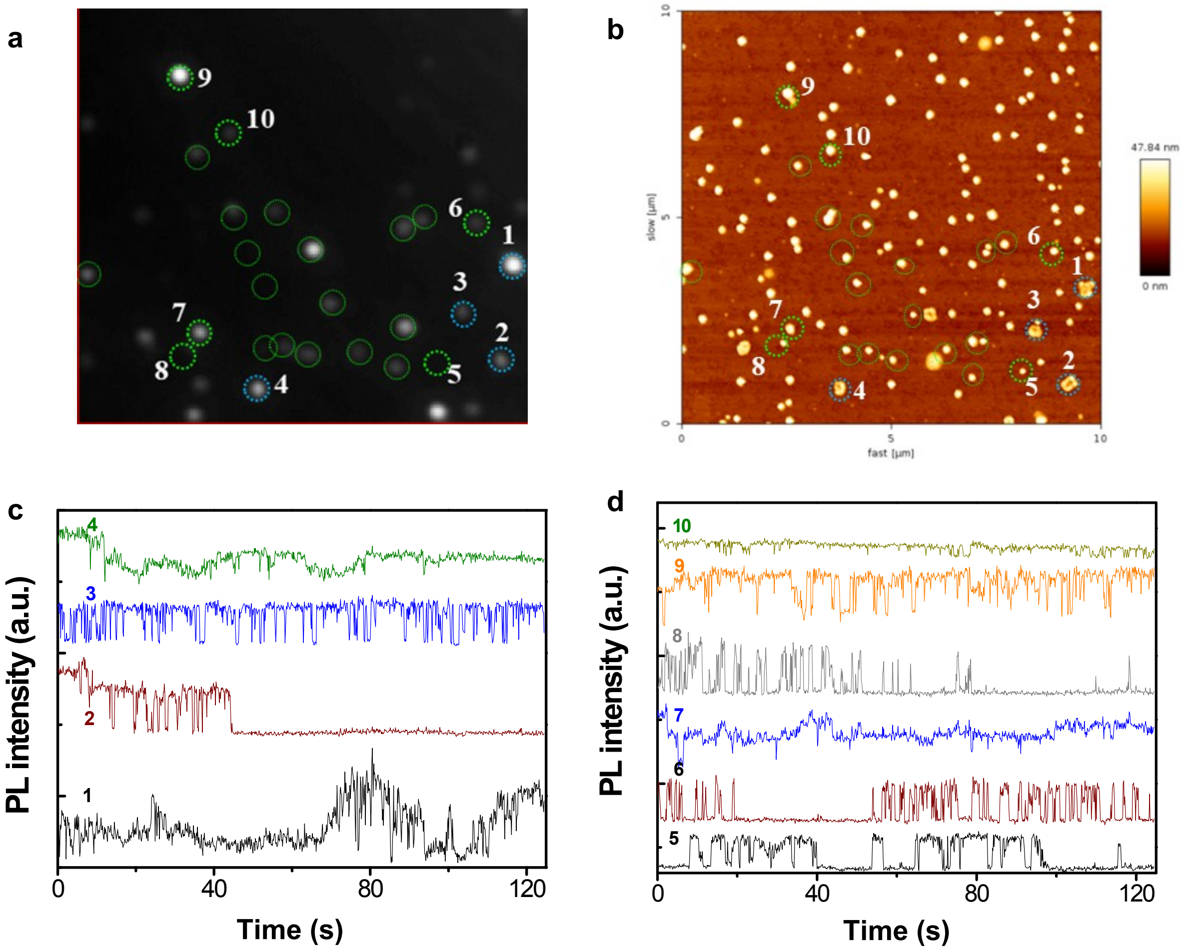

Figure S7. a,b) Correlative fluorescence and AFM images of single $cNP_{oligomer}$ with different morphology identified in blue and green circles. The dimensions of both images is 10 µm x 10 µm. c,d) Fluorescence intensity trajectories (124 ms/data point) of selected single $cNP_{oligomer}$ inside blue (1-4) and green dotted circle (5-10) in figure a and b.

Fluorescence lifetime imaging (FLIM).

The samples for FLIM measurement were prepared by drop casting of 100 µL of $MAPbBr_3$ in toluene on hydrophobic cover glass slide (Menzel-Gläser 22 mm x 22 mm). The sample was dried under saturated hexane atmosphere following the procedure describe previously for TEM sample preparation.

FLIM images were measured using an inverted-type scanning confocal microscope (Leica TCS SP8 SMD), with an oil immersion objective (Olympus 100 x) and at room temperature. A 488 nm pulsed diode laser (PicoQuant PDL 800-B) was used for excitation with repetition rates of 2.16 MHz. The emission was registered between 500-600 nm. Exponential fitting for the obtained fluorescence decays (extracted from the FLIM images) were performed using Symphotime software (version 6.0).

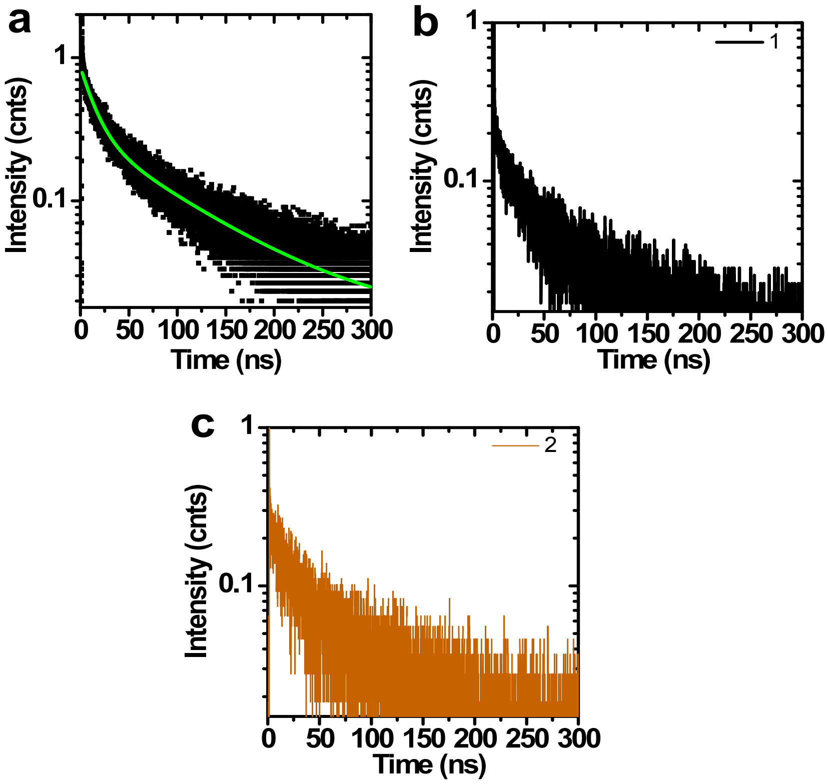

Figure S8. a) Representative time-resolved PL decays traces and b,c) Local PL time-resolved decay traces of selected region in FLIM image in figure 2e.

Table S2. Local PL decay parameters of different regions of FLIM image shown in Figure 3.

Position	τ_{av} **(ns)**	τ_1 **(ns)**	τ_2 **(ns)**	**A_1 (%)**	**A_2 (%)**
Overall image	**73.4**	13.8	90.1	65	35
Area 1	**64.4**	11.8	77.3	62	38
Area 2	**64.9**	13.5	78.6	61	39

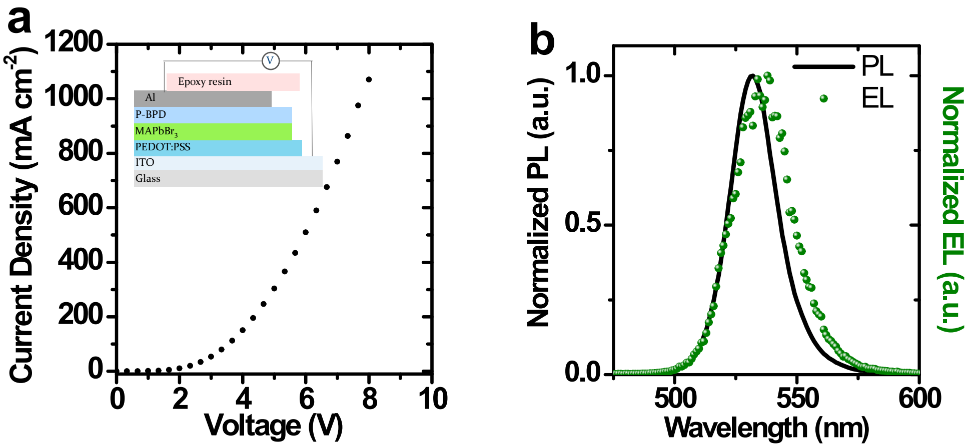

Figure S9. a) Current-density–voltage (J–V) curve of the electroluminescent device (ITO/PEDOT:PSS/ MAPbBr$_3$/PBD/Al), prepared from colloidal MAPbBr$_3$ nanoparticles. Inset: device structure. b) Room temperature electroluminescent spectrum of the de device (at 7 V); the black line represent the PL steady state spectrum.

References

1. M. Acik, I. K. Park, R. E. Koritala, G. Lee and R. A. Rosenberg, *Journal of Materials Chemistry A*, 2018, **6**, 1423-1442.
2. S. Gonzalez-Carrero, R. E. Galian and J. Perez-Prieto, *Journal of Materials Chemistry A*, 2015, **3**, 9187-9193.

3. H. Huang, J. Raith, S. V. Kershaw, S. Kalytchuk, O. Tomanec, L. Jing, A. S. Susha, R. Zboril and A. L. Rogach, *Nature Communications*, 2017, **8**, 996.
4. F. Zhang, H. Zhong, C. Chen, X.-g. Wu, X. Hu, H. Huang, J. Han, B. Zou and Y. Dong, *ACS Nano*, 2015, **9**, 4533-4542.
5. M. Lashkor, F. J. Rawson, J. A. Preece and P. M. Mendes, *Analyst*, 2014, **139**, 5400-5408.
6. A. Monserrate, S. Casado and C. Flors, *Chemphyschem*, 2014, **15**, 647-650.
7. P. Bondia, S. Casado and C. Flors, in *Super-Resolution Microscopy: Methods and Protocols*, ed. H. Erfle, Springer New York, New York, NY, 2017, DOI: 10.1007/978-1-4939-7265-4_9, pp. 105-113.